SU-8 etching in inductively coupled oxygen plasma

Rasmussen, Kristian Hagsted; Keller, Stephan Sylvest; Jensen, Flemming; Jørgensen, Anders Michael; Hansen, Ole

Published in:
Microelectronic Engineering

Link to article, DOI:
10.1016/j.mee.2013.05.011

Publication date:
2013

Document Version
Publisher's PDF, also known as Version of record

Microelectronic Engineering 112 (2013) 35–40

Contents lists available at SciVerse ScienceDirect

Microelectronic Engineering

journal homepage: www.elsevier.com/locate/mee

SU-8 etching in inductively coupled oxygen plasma ☆

Kristian Hagsted Rasmussen [a,*], Stephan Sylvest Keller [a], Flemming Jensen [b], Anders Michael Jorgensen [b], Ole Hansen [a,c]

[a] Department of Micro- and Nanotechnology, Technical University of Denmark, DTU Nanotech Building 345E, DK-2800 Kgs. Lyngby, Denmark
[b] DTU Danchip, Technical University of Denmark, Oersteds Plads Building 347, DK-2800 Kgs. Lyngby, Denmark
[c] CINF – Center for Individual Nanoparticle Functionality, Technical University of Denmark, DK-2800 Kgs. Lyngby, Denmark

ARTICLE INFO

Article history:
Received 1 February 2013
Received in revised form 9 April 2013
Accepted 16 May 2013
Available online 7 June 2013

Keywords:
Dry etching
ICP-RIE
SU-8
Antimony
Roughness
SF_6

ABSTRACT

Structuring or removal of the epoxy based, photo sensitive polymer SU-8 by inductively coupled plasma reactive ion etching (ICP-RIE) was investigated as a function of plasma chemistry, bias power, temperature, and pressure. In a pure oxygen plasma, surface accumulation of antimony from the photo-initiator introduced severe roughness and reduced etch rate significantly. Addition of SF_6 to the plasma chemistry reduced the antimony surface concentration with lower roughness and higher etch rate as an outcome. Furthermore the etch anisotropy could be tuned by controlling the bias power. Etch rates up to 800 nm min^{-1} could be achieved with low roughness and high anisotropy.

1. Introduction

SU-8 is an epoxy based, photo sensitive polymer developed by IBM in the late 1980s [1]. SU-8 negative photo resist is derived from EPON™resin [2], where the monomer consists in average of eight epoxy groups and eight aromatic benzene groups as indicated by the name. The viscous polymer contains between 5% and 10% photo-initiator enabling cross linking by standard I-line lithography. The photo-initiator used for the SU-8 resin is based on triarylsulfonium–hexafluoroantimonium, adding fluorine, sulfur, and antimony to the carbon, hydrogen, and oxygen from the monomers as elements in the SU-8 resin.

SU-8 in microtechnology was developed for use in LIGA[1] [3] where the polymer is used to define a structured mold. Furthermore, SU-8 was interesting as etch mask, due to the patterning by standard photolithography. The chemical resistance of SU-8, however, complicates the removal of the resist in both applications, with plasma removal as one of the only reliable option. Therefore, the most thoroughly discussed subject in SU-8 etching is complete removal of SU-8 after its use as masking material.

More recently, SU-8 has been used as a device layer rather than a sacrificial layer. Fabrication of devices in SU-8 can in general be accomplished by photo-lithography, for a large number of applications. Lab on a chip (LOC) systems with microfluidic channels made in SU-8 [4,5], have advantages such as biological compatibility and easy fabrication. Devices for optical applications such as polymer waveguides [6] and optical transducers [7] have been shown. Furthermore, the mechanical properties of SU-8 make it an obvious choice for cantilever sensors [8].

Plasma treatment of all of these devices can be used for several purposes. Probably the most relevant cases of plasma treatment of SU-8, in addition to removal, is functionalization or activation of a surface. This can for example be used to tune the hydrophobicity of a surface or change the surface termination to alter the bonding capabilities [9]. For some applications further patterning of the SU-8 after the initial photo-lithography in the form of etching might be interesting. For instance an isotropic etch can be used to increase the aspect ratio or decrease the line width of lithographically defined structures.

In the scarce literature on SU-8 etching available, most authors agree on the need for fluorine in the plasma chemistry. However, there has not been offered a satisfying explanation for this observation.

Dentinger et al. [10] presented a study on different methods for SU-8 removal, including removal using solvents, chemical removal

* Corresponding author. Address: Building 344, Room No. 208, Oersteds Plads, DK-2800 Kgs. Lyngby, Denmark. Tel.: +45 4525 5848; fax: +45 4588 7762.
E-mail addresses: khara@nanotech.dtu.dk, kristian.rasmussen@nanotech.dtu.dk (K.H. Rasmussen).

[1] Lithographie, Galvanoformung, Abformung.

0167-9317/$ - see front matter © 2013 The Authors. Published by Elsevier B.V. All rights reserved.
http://dx.doi.org/10.1016/j.mee.2013.05.011

in different plasma etching configurations, and other more exotic methods. For our study the chemical removal in any type of plasma setting is interesting. Both, results from reactive ion etching (RIE) as well as downstream chemical etching (DCE) can increase the understanding of the different mechanism involved in the process. Etch rates of 1–4 μm min^{-1} were obtained in RIE using a mixture of CF_4/O_2 in approximately equal proportions [10].

In DCE, Dentinger et al. observed that only 2–4% of CF_4 was needed to obtain etch rates as high as 10 μm min^{-1}. However, to obtain such high rates the temperature was elevated to 275 °C. Such high temperatures will introduce thermal stress in the polymer, increasing the risk of cracking and peeling. It will also cause compatibility problems with some materials in practical applications. Furthermore, surface contamination with antimony was observed after complete SU-8 removal. Dentinger et al. ascribed the surface antimony contamination to residues left from the photo initiator.

The influence of fluorine on etching of cured SU-8 is also discussed by Hong et al. [11] and Mischke et al. [12]. Mischke et al. used CF_4 just as Dentinger et al. did, while Hong et al. added SF_6 as fluorine source to the plasma. Hong et al. limit the discussion to etch rate and anisotropy without discussing chemical composition. However Mischke et al. [12] used Energy-dispersive X-ray spectroscopy (EDX) on etched SU-8 surfaces to identify antimony and fluorine in addition to the expected carbon and oxygen. Mischke et al. conclude that fluorine is introduced by the etch chemistry, neglecting the fact that the photo initiator in SU-8 is triarylsulfonium hexafluorantimonium which includes SbF_6^+ ions.

De Volder et al. [13] used plasma etching to produce nanowires in SU-8. Their process is basically an oxygen plasma etch where they also see an accumulation of antimony at the surface; the antimony is believed to act as local masking agent and starting point of the nanowires. X-ray photoelectron spectroscopy (XPS) analysis of the surface shows up to 19%$_{atom}$ antimony surface concentration in their experiments. Similar to Mischke et al. no external source for antimony was present, and the antimony must hence originate from the SU-8 photo-initiator. For removal of SU-8 this will result in rough surfaces and low etch rates and should be avoided.

The presence of antimony in plasma treated surfaces is a problem for biological applications since antimony is toxic. This does not only apply to samples structured by plasma etching, but also surfaces cleaned or primed in an oxygen plasma will have increased concentrations of antimony in the surface after a shallow etch. Small amounts of antimony may not be critical since the toxicity is weaker than e.g. that of arsenic [14,15]. However, since etching generates thin hairlike structures it can be assumed that the antimony present in the surface is on nanometer scale, for which Bregoli et al. [16] has evaluated the toxicity and found it poisonous. It is important to minimize the antimony concentration to achieve relevant results for biological experiments performed on SU-8 chips.

In this work we will discuss structuring of SU-8 in an ICP-RIE oxygen plasma with varying SF_6 content. Control of antimony concentration and surface roughness will be discussed, together with measurements of etch anisotropy and rate. We will in more detail discuss the influence of antimony on the surface quality obtained and link it to the etch chemistry.

2. Experimental

All SU-8 etching experiments were done in a turbo pumped, inductively coupled plasma (ICP) system, Advanced Silicon Etcher (ASE HC250M) from STS, refitted for polymer etching. The system is fitted with two RF power supplies; the main power supply, the Coil Power, controls the intensity of the plasma, while the secondary power supply, the Bias Power, controls the ion energy of the ion flux to the etched substrate. In the experiments reported here, the feed gasses oxygen (O_2) and sulfur hexafluoride (SF_6) were used at flow rates controlled using mass flow controllers. The pressure in the etch chamber is controlled by a throttle valve and measured using a pressure gauge. All sample preparation and characterization except XPS was carried out in a cleanroom environment.

Since plasma etching, in general, is a very complicated process involving many parameters, Design of Experiments (DoE) was used to reduce the number of experiments necessary to identify the most important parameter relations in etching of SU-8.

2.1. Design of experiments

The number of experiments conducted was reduced by selecting the four most important parameters for variation, Table 1 while the remaining parameters were kept constant. The O_2 flow rate (Q_{O_2}) was keep constant at 99 sccm, while the SF_6 flow rate (Q_{SF_6}) was varied between 0 and 20 sccm. The pressure in the etch chamber was controlled to keep the gas density stable. Since the pressure has a pronounced effect on etch characteristics, the pressure (p) was varied between 20 and 40 mTorr. It should be noted that the system was run in automatic pressure control mode, which continuously adjusts the throttle valve to keep a constant pressure during etch. The coil power (P_C) was fixed at 1000 W, while the bias power (P_B) was varied between 0 and 30 W. Finally, the substrate chuck temperature (T) was controlled between 10 and 50 °C. This design resulted in a full factorial screening in four parameters, where three center points were used to check for quadratic curvature, where the quadratic term of a parameter is needed to generate a valid model. The total number of experiments in this setup is 19, which were processed for 20 min each. The experiments in the design were carried out in random order.

After completion of the first set of experiments it was evident that curvature was present in the response. To enable data analysis and generation of a valid model for the system, the curvature was addressed by adding eight face centered points with two additional center points to the design. A face centered point is a center point with one parameter value at min or max. The ten extra experiments were also carried out in random order, and the center points were used to check for variations between the two sets of experiments. The final dataset comprises the 19 initial experiments combined with the 10 additional, giving a total of 29 experiments to characterize.

2.2. Sample preparation

Samples were prepared by spinning 25 μm SU-8 2075 resist on 100 mm silicon wafers with a 2 μm thick thermal silicon dioxide followed by 1 h of baking on a hotplate at 50 °C [17]. The samples were exposed with 150 mJ cm^{-2} at the I-line, through a test mask with line arrays of different widths, and baked for 2 h at 50 °C on a hotplate, followed by development in PGMEA. Finally, to completely crosslink the polymer, samples were flood exposed

Table 1
Parameters used for DoE design. Center denotes the value used for center points and face centered points.

Parameter		Min	Center	Max
Coded value		−1	0	1
SF_6 flow rate (sccm)	Q_{SF_6}	0	10	20
Pressure (mTorr)	p	20	30	40
Bias power (W)	P_B	0	15	30
Temperature (°C)	T	10	30	50

with 500 mJ cm^{-2} at the I-line and baked for 15 h at 90 °C in an oven. The sample patterning by photo lithography facilitated characterization of the subsequent etch. Prior to each etch experiment the chamber was conditioned using a 20 min chamber clean in an oxygen plasma with a blank silicon wafer loaded. For the cleaning process, the chuck temperature was always set at 20 °C. The chamber cleaning process was considered necessary to ensure stable and predictable conditions in each etch process, since the condition of the chamber walls might affect plasma etching processes. When a new substrate was loaded for etching, the temperature was set to the required value and allowed to stabilize before the etch experiment was started.

2.3. Characterization

Before and after etching, the samples were characterized with respect to etched depth, structure width, surface morphology, and composition. The height of the structures was measured before and after etching using a Dektak 8 stylus profiler from Veeco. Scanning electron microscopy (SEM) images were used to characterize the structure width and the appearance of the surfaces. The width of the structures found from SEM images and the known line pitch in the line array were used to characterize line width reduction during the etch process. For line width measurements, lines in the center of the arrays were chosen to eliminate influence of RIE loading effects on the line width. The roughness was measured using atomic force microscopy (AFM) after etching.

The surface composition of the samples was characterized using XPS. The analysis was carried out in a Thermo K-Alpha XPS instrument with a monochromatic Al–Kα-source and charge compensation. For each sample a binding energy survey from 0 to 1350 eV was performed followed by detailed spectra analysis in the O1s, Sb3d, F1s, and C1s binding energy ranges. The atomic concentrations of surface elements were extracted using the software package Advantage provided by Thermo. In the calculations for the O1s and Sb3d peaks, the ratio and separation of antimony peaks $Sb3d_{3/2}$ and $Sb3d_{5/2}$ were fixed to 0.577 [18] and 9.34 eV [19], respectively. By doing this it was possible to find the surface concentrations of the four main elements in the surface layer: C, O, F, and Sb.

3. Results and discussion

The etch outcome was evaluated on four different parameters. Etch rate (r) and anisotropy (A) are important parameters for controlling etch depth and profile in etching. Furthermore, since severe roughening of the surface was observed after etch, root mean square surface roughness (R_{rms}) and surface composition were measured by AFM and XPS. The surface composition was found as the fractional atomic content of carbon [C], oxygen [O], fluorine [F], and antimony [Sb] in the polymer surface layer. All results outlined below are extracted from the total set of 29 experiments.

The DoE was used to find parameters and interactions with a 0.05 level of significance. Parameters with a significant interaction or quadratic term were always included, even if it's P-value was above 0.05. In Table 2 the P-values are listed for the four measured responses, [Sb], r, A, and R_{rms}. Some interactions and quadratic terms were insignificant for all responses and are not included in the tables. The coefficients of determination (R^2) for the final models are listed in the last row of Table 2.

The etch outcome can be estimated for a response y by a DoE fitted model as,

$$y_i = \beta_i + \sum_j \beta_{ij} x_j + \sum_{j,k} \beta_{ijk} x_j x_k. \quad (1)$$

Table 2
P-values of the DoE fit. Fitting a model for the responses with DoE results in the following P-values, with parameters that were negligible removed. If no value is given for a parameter or interaction it was excluded from the model. The four measured responses are Sb concentration ([Sb]), etch rate (r), anisotropy (A), and root mean square roughness (R_{rms}).

Term	P ([Sb])	P (r)	P (A)	P (R_{rms})
Q_{SF_6}	$< 10^{-4}$	0.6[a]	0.43a	$< 10^{-4}$
T	0.1a	0.006	–	–
P_B	0.005	$< 10^{-4}$	$< 10^{-4}$	$< 10^{-4}$
p	–	$< 10^{-4}$	0.0001	–
$(Q_{SF_6})(T)$	0.02	–	–	–
$(Q_{\nu})(P_B)$	0.0007	0.03	0.0005	$< 10^{-4}$
$(Q_{SF_6})^2$	$< 10^{-4}$	$< 10^{-4}$	–	$< 10^{-4}$
$(P_B)(p)$	–	0.0002	0.006	–
$(P_B)^2$	–	0.009	0.004	–
R^2	0.94	0.97	0.90	0.93

[a] Included since interactions are significant.

x and y denotes the DoE coded parameters and the response respectively, and $\beta_{i(jk)}$ denotes the estimated coefficients listed in Table 3. The index i denotes the response, while indices j and k denote the parameters.

3.1. Antimony surface concentration

The antimony surface concentration was estimated by XPS spectra of each sample, see Fig. 1. XPS survey spectra revealed that C, O, F, and Sb were the only measurable elements in the SU-8 surface layer, which is in agreement with the known elemental composition of the photo resist [1], if it is assumed that S reacts in the plasma and leaves the surface during etch. The detailed spectra shown in Fig. 1 are therefore shown for binding energies relevant for these elements. Only traces of antimony were observed in the surface layer of non-etched SU-8. SU-8 with 5% photo-initiator contains approximately 0.05%$_{atom}$ antimony which is below the detection limit. For etched SU-8, the amount of antimony measured in the surface layer increased significantly, indicating an antimony accumulation during etch.

The XPS measurements of surface elements showed that the antimony surface concentration was highly dependent on the SF_6 flow rate to both first and second order. In Fig. 2a it is evident that the antimony concentration drastically decreased when SF_6 was added to the plasma. The same tendency is obvious on the contour

Table 3
DoE fit of dependencies. Fitting a model for the responses with DoE gives the following dependencies. Values between columns should not be compared. If no value is given for a parameter or interaction it was excluded from the model. The four measured responses are Sb concentration ([Sb]), etch rate (r), anisotropy (A), and root mean square roughness (R_{rms}).

$\beta_{i(jk)}$	[Sb] (%$_{atom}$)	r (μ min^{-1})	A	R_{rms} (nm)
β_i	2.5	9.57	0.56	9.47[a]
$\beta_{i(Q_{\nu})}$	−8.1	−0.08	−0.02	−208
$\beta_{i(T)}$	0.9	0.49	–	–
$\beta_{i(P_B)}$	1.7	2.93	0.31	144
$\beta_{i(p)}$	–	−1.25	−0.12	–
$\beta_{i(Q_{SF_6})(T)}$	−1.4	–	–	–
$\beta_{i(Q_{\nu})(P_B)}$	−2.2	0.38	0.11	−166
$\beta_{Q_{SF6}}{}^2$	7.6	−3.8	–	207
$\beta_{i(P_B)(p)}$	–	−0.77	0.08	–
$\beta_{i(P\|ofortt\|B\|cfortt\|)^2}$	–	−1.05	−0.13	–

[a] Intercept was negligible, but included in model.

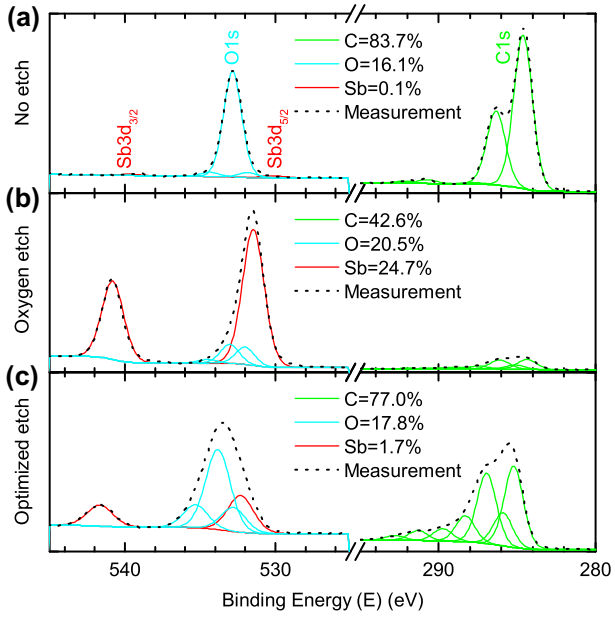

Fig. 1. XPS measurements on processed SU-8 surfaces. Surveys of all samples showed that C, O, Sb, and F were the only elements in the polymer surface. The spectrum analysis showed four different carbon bonds, shown as green curves. Oxygen and antimony were discerned by fixing the ratio of distance and size between the $Sb3d_{5/2}$ peak to the $Sb3d_{3/2}$ peak to fit the $Sb3d_{5/2}$ while O2s was fitted for the remaining area. The oxygen contribution was divided in two types of carbon bonds. Fluorine spectra are not shown, but two bonds for fluorine were used to find the total atomic concentration. Etching of both (b) and (c) were done at $P_C = 1000$ W, $P_B = 30$ W, and $Q_{O_2} = 99$ sccm. For (b) $p = 20$ mTorr, $T = 10$ °C, and $Q_{SF_6} = 0$ sccm was used, while for (c) $p = 40$ mTorr, $T = 30$ °C and $Q_{O_2} = 17$ sccm was used.

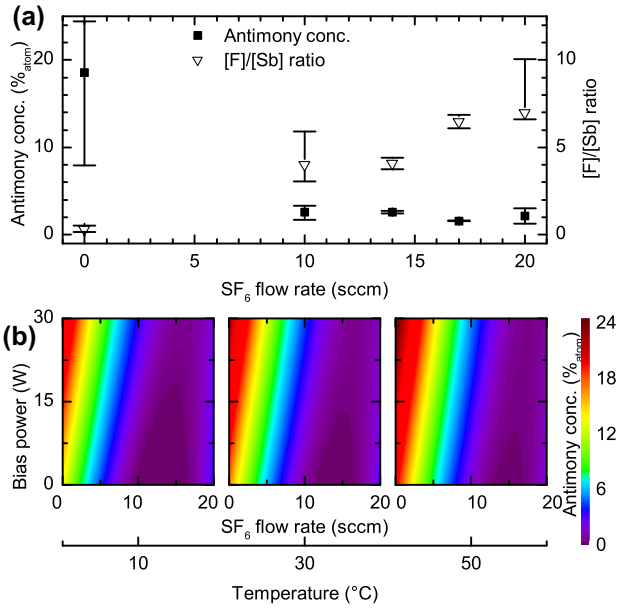

Fig. 2. Antimony surface concentration ([Sb]) as a function of relevant etch parameters. [Sb] and [F]/[Sb] ratio were highly dependent on Q_{SF_6}. (a) Low Q_{SF_6} caused high [Sb] while the [F]/[Sb] ratio became low. (b) [Sb] was primarily dependent on Q_{SF_6} but also T and P_B while p did not show any influence on [Sb].

plots shown in Fig. 2b, independent of the other parameters. Moreover the [F]/[Sb] ratio, also shown in Fig. 2a, increased from below one to three or more. This indicates that most fluorine from the photo initiator desorbed from the surface if fluorine was not added to the gas phase.

For samples etched at low SF_6 flow, the [F]/[Sb] ratio was much lower than the expected six that should be present considering the catalyst stoichiometry. The low ratio suggests that the SbF_6^+ ion reacts in the plasma to form other antimony compounds such as atomic antimony or antimony oxides. Atomic antimony and antimony oxide both have high boiling points of 1587 and 1425 °C [20]. Hence low vapor pressures of antimony and antimony oxides are expected at the processing temperatures used and antimony is expected to stay on the surface. For samples processed at high SF_6 flow rate, fluorinated compounds are expected on the surface. Antimony trifluoride and pentafluoride have boiling points of 376 and 141 °C [20], and in consequence much higher vapor pressures at the processing temperatures. Therefore, these compounds are more likely to evaporate from the surface, resulting in low antimony concentration and a [F]/[Sb] ratio close to the one of the photo-initiator.

Bias power as well as first order interaction with SF_6 flow rate also had an effect on the antimony surface concentration, with higher bias power resulting in higher antimony concentrations. This might be ascribed to ion-enhanced etching [21] with more active sites generated on the polymer backbone. Consequently the polymer etch rate may increase more than the antimony etch rate resulting in a faster antimony accumulation. However the increased antimony accumulation rate could be alleviated by adding more SF_6 to the plasma.

Antimony surface concentration only showed a small dependency on temperature. The antimony surface concentration increased at elevated temperatures. This may be explained by an increase in polymer etch rate for higher temperatures. In other words, the rate of antimony removal is slower than the polymer etch rate. The pressure was found to not influence the antimony concentration.

3.2. SU-8 etch rate

Specific etch depths are usually obtained by control of the etch duration and hence the etch rate must be known. Our experiments showed a dependency of the etch rate on all parameters, see Fig. 3.

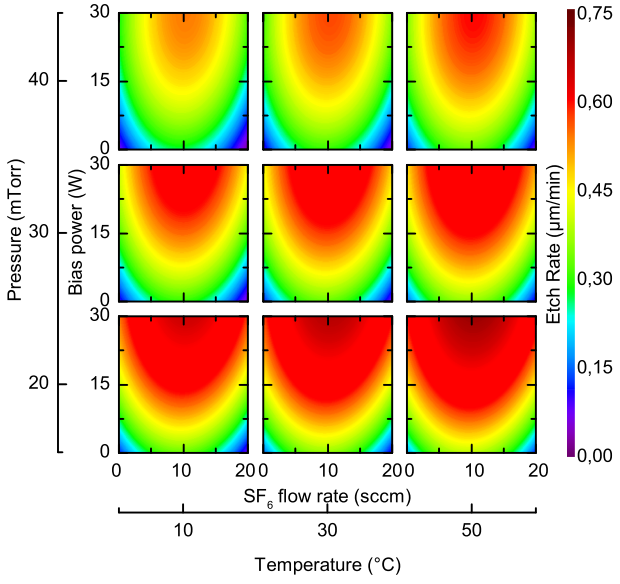

Fig. 3. Etch rate (r) as a function of etch parameters. Etch rate showed a dependency on all parameters. Q_{SF_6} and P_B both have a strong influence on etch rate. p also affected the etch rate significantly with higher p resulting in lower etch rates. T only slightly influences etch rate and does not interact with any of the other parameters.

The most notable dependency was on bias power which controls the ion energy during etch. Increased bias power led to faster etching, either due to sputtering or more likely ion-enhanced etching [21]. Supporting the hypothesis of ion-enhanced etching, the gain in etch rate was more significant for low bias powers.

The SF_6 flow rate to the second order, also significantly affected the etch rate. The response showed curvature with reduced etch rate for both high and low SF_6 flow rates. For low SF_6 flow rates antimony accumulates at the surface, resulting in partial masking of the surface which reduces the etch rate. The decrease in etch rate at higher SF_6 flow rates might be explained by reactions between SF_5 radicals and O, which will reduce the amount of reactive oxygen available for the polymer etch.

Higher pressure in general reduced the etch rate. Interaction between pressure and bias power slightly influenced this tendency. The change in etch rate due to the interaction was most pronounced at high bias powers, while for lower bias power the effect of pressure on etch rate decreased. The decreased etch rate at higher pressures may be due to dilution of plasma species, decreased ion sputtering due to lower mean free path and lower ion energy, or a combination.

Finally, the substrate temperature also influenced the etch rate. Higher temperature increased the etch rates due to thermal activation and higher vapor pressures. Temperature was the only parameter on which etch rate exhibited a linear dependency within the parameter space, while all other parameters interacted with bias power.

In Fig. 3 an overview of the influence of the four parameters on etch rate is shown. From the graphs it is obvious that high bias power and medium SF_6 flow rate give the highest etch rates.

3.3. Etch anisotropy

In addition to etch rate, control of etch anisotropy is important for optimal pattern transfer. The etch anisotropy was calculated as $A = 1 - r_L/r$ where r_L is the lateral etch rate. It was observed that bias power had the largest effect on the anisotropy of the etch, see Fig. 4. As expected increased bias power improved the etch anisotropy due to higher ion energy and thus improved directionality of the etch.

Pressure also influenced etch anisotropy, and a weak interaction between bias power and pressure was evident. At higher pressures the etch was more isotropic due to the reduction of the mean free path in the plasma and hence reduced ion energy and directionality.

The interaction between the SF_6 flow rate and the bias power was significant. However, as seen in Fig. 4, for both anisotropic and isotropic etching high SF_6 flow rate was optimal. SF_6 can introduce more directionality by adding more heavy, charged particles to the plasma body. However SF_6 does not only add charged particles, but also heavy non charged particles, which limits the directionality. Hence bias power determines the shift from one regime to the other. High bias power is necessary to maintain high anisotropy when the SF_6 flow rate is increased.

Etch anisotropy did not show any dependency on temperature.

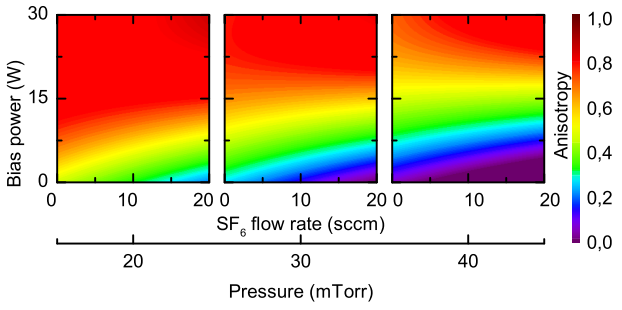

Fig. 4. Etch anisotropy (A) as a function of etch parameters. The anisotropy showed no dependency on the T, whereas the three other parameters all influenced the outcome. Of notice is the dependency on Q_{SF_6} as both for isotropic and anisotropic etches high Q_{SF_6} gives the best result.

3.4. Roughness

The surface roughness is primarily controlled by the SF_6 flow rate, with decreased roughness as a response to more fluorine in the plasma. The SF_6 flow rate affects the roughness response to both first and second order. The interaction between the SF_6 flow rate and bias power, and bias power to first order also influenced the roughness, with increased roughness at higher bias power. The nature of the dependencies on SF_6 flow rate and bias power, indicates that roughness and antimony surface concentration are closely linked. In Fig. 5a the roughness is plotted against the antimony concentration, and a clear tendency is detected such that if the antimony concentration is kept low, the roughness will also be low.

It is worth noticing that for low roughness the [F]/[Sb] ratio in the surface layer is high. Comparing the [F]/[Sb] ratio with the Sb concentration indicates a threshold at which the amount of fluorine in the surface layer is enough to generate volatile antimony compounds. From Fig. 5a it seems that a ratio of [F]/[Sb] of 3:1 enables the antimony to start leaving the surface. This correlates fine with the hypothesis that SbF_3 and SbF_5 may be the volatile compounds formed.

The contour plot in Fig. 5b of the influence of the different parameters on surface roughness shows the same tendencies as for antimony concentration. However, the interaction between bias power and SF_6 flow rate is more pronounced for roughness than antimony surface concentration. From the contour plot it is clear that the roughness can become quite high. The high surface roughness was visible with the naked eye as a dull surface, and in SEM pictures it is readily identified. Fig. 6b shows a sample

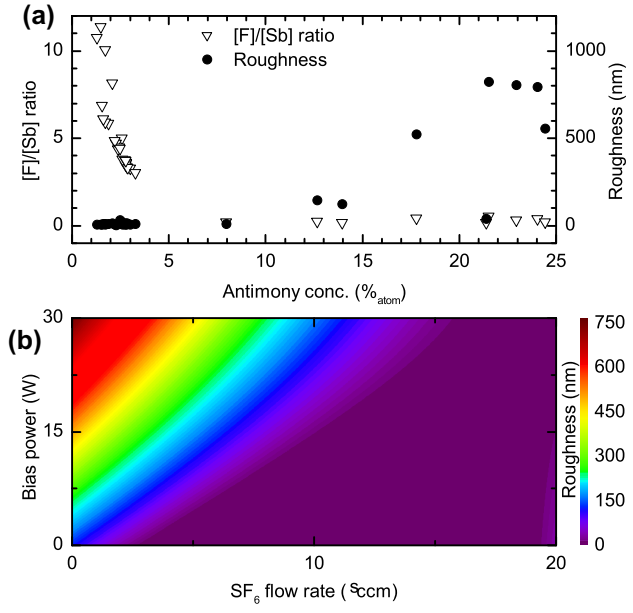

Fig. 5. Root mean square surface roughness (R_{rms}) as a function of relevant etch parameters and R_{rms} and [Sb] concentration correlations. (a) Low [Sb] ensure low R_{rms}, note, that to reach low [Sb] [F] has to be relatively high. (b) The roughness contour shows similar tendencies as the antimony response, however T did not have and effect on R_{rms} just as p also does not.

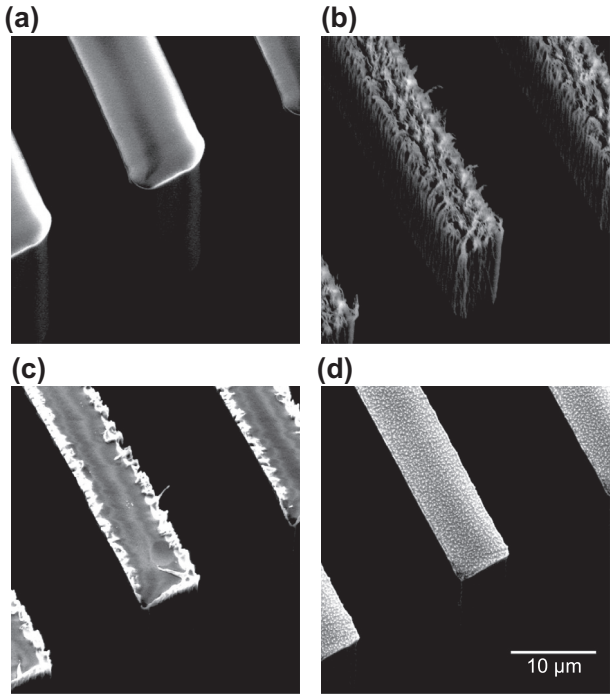

Fig. 6. Surface topology of etched samples. (a) A wafer just after development of the SU-8 layer. (b) The pure oxygen plasma (P_B=30 W, T = 10 °C, p = 20 mTorr, Q_{SF_6} = 0 sccm) causes a high roughness. (c) Optimized etch (P_B=30 W, T = 30 °C, p = 40 mTorr, Q_{ν} = 17 sccm) with high anisotropy at reasonable etch rate and with a smooth surface. (d) Optimized etch (P_B = 0 W, T = 10 °C, p = 20 mTorr, Q_{SF_6} = 14 sccm) at low anisotropy with moderate etch rate and a smooth surface.

etched in a pure oxygen plasma; this sample has a high roughness compared to that of a non-etched sample as shown in Fig. 6a. In Fig. 6c and 6d two samples etched with optimized parameters for low roughness are shown. The two etch processes were optimized for different anisotropy; in Fig. 6c the anisotropy is 0.9 while in Fig. 6d the anisotropy is 0.3. This gives a good indication that relatively smooth surfaces can be obtained with both high and low anisotropy.

Sidewall and edge roughness as seen in Fig. 6c were linked directly to the bias power, with generation of edge roughness when a non zero bias power was applied. The dependency on bias power suggest that sidewall roughness is an effect of plasma directionality. For highly anisotropic etches antimony fluoride desorption on vertical surfaces is not assisted by ion bombardment. For samples etched with no bias power the absence of roughness can be explained by the lower etch rate for these samples. Samples with rough sidewalls always showed rough edges.

4. Conclusion

A DoE study of SU-8 plasma etching enabled improved control of surface properties of the polymer. For a pure oxygen plasma, high antimony concentration, high roughness, and low etch rate were observed. The amount of antimony accumulated at the surface could be reduced to a few percent by addition of SF_6 to the oxygen plasma, which directly lowered the surface roughness. Reasonable etch rates up to 0.8 μm min^{-1} could be obtained at high anisotropy, while optimizing for an isotropic etch will inevitable cause a reduction of the etch rate.

The high concentration of antimony accumulated at the surface must be considered when SU-8 devices are to be used for biological application. For short plasma treatments the antimony concentration will not increase much, but if samples are processed for longer times it will definitely be an issue. For complete removal of the SU-8 antimony surface accumulation results in a contaminated surface. However, adding SF_6 to the plasma chemistry can minimize the residue level and improve the usability of SU-8 as sacrificial mask.

Acknowledgment

CINF – Center for Individual Nanoparticle Functionality is supported by the Danish National Research Foundation.

References

[1] J.D. Gelorme, R.J. Cox, S.A.R. Gutierrez, Photoresist composition and printed circuit boards and packages made therewith, Patent, US 4882245 (11) 1989.
[2] Momentive Specialty Chemicals Inc., EPON™ resin SU-8 (a.k.a. EPIKOTE™157), Web. 8 January 2013 (September) 2001. http://www.momentive.com/Products/TechnicalDataSheet.aspx?id=3603
[3] K.Y. Lee, N. LaBianca, S.A. Rishton, S. Zolgharnain, J.D. Gelorme, J. Shaw, T.H.P. Chang, J. Vac. Sci. Technol. B 13 (6) (1995) 3012, http://dx.doi.org/10.1116/1.588297.
[4] L. Guerin, M. Bossel, M. Demierre, S. Calmes, P. Renaud, in: Transducers 97, vol. 2, IEEE, Chicago, 1997, pp. 1419–1422, http://dx.doi.org/10.1109/SENSOR.1997.635730.
[5] R.J. Jackman, T.M. Floyd, R. Ghodssi, M.A. Schmidt, K.F. Jensen, J. Micromech. Microeng. 11 (3) (2001) 263–269, http://dx.doi.org/10.1088/0960-1317/11/3/316.
[6] K.B. Mogensen, J. El-Ali, A. Wolff, J.P. Kutter, Appl. Opt. 42 (19) (2003) 4072, http://dx.doi.org/10.1364/AO.42.004072.
[7] S. Balslev, A.M. Jorgensen, B. Bilenberg, K.B. Mogensen, D. Snakenborg, O. Geschke, J.P. Kutter, A. Kristensen, Lab. Chip. 6 (2) (2006) 213, http://dx.doi.org/10.1039/b512546d.
[8] M. Nordström, S. Keller, M. Lillemose, A. Johansson, S. Dohn, D. Haefliger, G. Blagoi, M. Havsteen-Jakobsen, A. Boisen, Sensors 8 (3) (2008) 1595–1612, http://dx.doi.org/10.3390/s8031595.
[9] F. Walther, T. Drobek, A.M. Gigler, M. Hennemeyer, M. Kaiser, H. Herberg, T. Shimitsu, G.E. Morfill, R.W. Stark, Surf. Interface Anal. 42 (12-13) (2010) 1735–1744, http://dx.doi.org/10.1002/sia.3515.
[10] P.M. Dentinger, W.M. Clift, S.H. Goods, Microelectron. Eng. 61-62 (2002) 993–1000, http://dx.doi.org/10.1016/S0167-9317(02)00490-2.
[11] G. Hong, A. Holmes, M. Heaton, Microsys. Technol. 10 (5) (2004) 357–359, http://dx.doi.org/10.1007/s00542-004-0413-4.
[12] H. Mischke, G. Gruetzner, M. Shaw, Plasma etching of polymers like SU8 and BCB, in: J.A. Yasaitis, M.A. PerezMaher, J.M. Karam (Eds.), Micromachining and Microfabrication Process Technology VIII, Vol. 4979 of Proceedings of the Society of Photo-optical Instrumentation Engineers (SPIE), SPIE, 2003, pp. 372–381. doi: http://dx.doi.org/10.1117/12.472734.
[13] M.F.L. De Volder, R. Vansweevelt, P. Wagner, D. Reynaerts, C. Van Hoof, A.J. Hart, ACS Nano 5 (8) (2011) 6593–6600, http://dx.doi.org/10.1021/nn201976d.
[14] T. Gebel, Chem. Biol. Interact. 107 (3) (1997) 131–144, http://dx.doi.org/10.1016/S0009-2797(97)00087-2.
[15] K. Kuroda, G. Endo, A. Okamoto, Y.S. Yoo, S.-i. Horiguchi, Mutat. Res. Lett. 264 (4) (1991) 163–170, http://dx.doi.org/10.1016/0165-7992(91)90072-C.
[16] L. Bregoli, F. Chiarini, A. Gambarelli, G. Sighinolfi, A.M. Gatti, P. Santi, A.M. Martelli, L. Cocco, Toxicology 262 (2) (2009) 121–129, http://dx.doi.org/10.1016/j.tox.2009.05.017.
[17] L. Amato, S.S. Keller, A. Heiskanen, M. Dimaki, J. Emnéus, A. Boisen, M. Tenje, Microelectron. Eng. 98 (2012) 483–487, http://dx.doi.org/10.1016/j.mee.2012.07.092.
[18] T. Honma, R. Sato, Y. Benino, T. Komatsu, V. Dimitrov, J. Non-Cryst. Solids 272 (1) (2000) 1–13, http://dx.doi.org/10.1016/S0022-3093(00)00156-3.
[19] J.F. Moulder, J. Chastain, Handbook of X-ray Photoelectron Spectroscopy: A Reference Book of Standard Spectra for Identification and Interpretation of XPS Data, Physical Electronics Division, Perkin-Elmer Corp., Eden Prairie, MN, 1992.
[20] W.M. Haynes, CRC Handbook of Chemistry and Physics: A Ready-Reference Book of Chemical and Physical Data, 93rd ed., CRC Press/Taylor & Francis, Boca Raton, FL, 2012.
[21] J.D. Plummer, M. Deal, P.B. Griffin, Silicon VLSI Technology: Fundamentals, Practice and Modeling, Prentice Hall, Upper Saddle River, 2000.